# Demonstration of a microwave spectrum analyzer based on time-domain optical processing in fiber

**Robert E. Saperstein, Dmitriy Panasenko, and Yeshaiahu Fainman**

*Department of Electrical and Computer Engineering, University of California, San Diego, 9500 Gilman Drive, La Jolla, California 92093-0407*

Received July 18, 2003

We demonstrate a novel method for spectral analysis of microwave signals that employs time-domain processing in fiber. We use anomalous dispersion in single-mode fiber to perform a Fresnel transform followed by a matched amount of dispersion-compensating fiber to perform an inverse Fresnel transform of an ultrashort pulse. After the Fresnel-transformed waveform is modulated by the microwave signal, the waveform at the output of the dispersion-compensating fiber represents the ultrashort pulse convolved with the microwave spectrum. An experimental system for spectral analysis of microwave signals in the range 6–21 GHz is demonstrated. © 2004 Optical Society of America

*OCIS codes:* 070.1170, 320.7090, 300.6370.

Spectral analysis of high-energy microwave radiation in the gigahertz-to-terahertz range is essential for the investigation of signatures in such applications as radar, lidar, astronomical detection, imaging, and short-distance communication.[1–3] The bandwidths of conventional methods for frequency analysis depend on the speed of the electronics utilized. For high-resolution spectral analysis of large bandwidth signals, high-frequency mixers are employed to achieve channelization, leading to increased complexity and high power consumption. A useful alternative for the analysis of such signals is provided by techniques based on microwave photonics. For example, a microwave spectrum analyzer based on spectral hole burning achieves wide-bandwidth operation (10 GHz) with high spectral resolution (500 kHz).[4] However, because the spectral hole burning method fundamentally operates at low temperatures, its practical applications are limited. We demonstrate a novel method of direct frequency-domain spectrum analysis that relies on the manipulation of microwave-modulated ultrashort optical pulses by chromatic dispersion. Our research aims to create a robust room-temperature microwave spectrum analyzer by use of commercial all-fiber light-wave equipment with applicability into the submillimeter spectral range and with potential for megahertz-scale resolution.

Chromatic dispersion in fiber can be exploited to perform linear signal processing of propagating optical signals.[5] Specifically, Fourier transforms (FTs) are achieved in fiber by use of the chirp transform algorithm. In this method a phase modulator creates a time lens, and dispersive propagation leads to a FT of the signal at the back focal point of this time lens.[6] One can avoid the complexity of using the chirp transform algorithm, including a phase modulator, to make a FT by noting the mathematical analogy between the temporal effects of strong chromatic dispersion and the spatial effects of Fraunhofer diffraction.[7] The mapping of spectral components to time or space changes from a Fresnel transform (FrT) to an approximate FT as propagating signals reach the so-called far-field approximation. After a signal travels a sufficient distance in a fiber, its time waveform closely resembles the shape of its spectrum.[8] Here we demonstrate a novel approach to microwave spectrum analysis based on performing temporal FrTs of an ultrashort pulse in optical fiber. The operation of our method is shown schematically in Fig. 1. We use anomalous dispersion in single-mode fiber (SMF) to perform a FrT, followed by a matched amount of inverse dispersion in dispersion-compensating fiber (DCF) to perform an inverse FrT of an ultrashort pulse. The FrT field is transmitted through an electro-optic (EO) modulator driven by a microwave signal to be analyzed. The waveform at the output of the DCF is proportional to the ultrashort pulse convolved with the microwave spectrum.

The operation of the microwave spectrum analyzer can be described analytically as that of an ultrashort pulse transmitted sequentially through the SMF, the EO modulator, and the DCF. As the ultrafast pulse propagates through the SMF link, chromatic dispersion in the time domain leads to its broadening, described by the convolution of the ultrashort pulse with a quadratic phase factor. An input ultrafast waveform, $U(0,t)$, will be represented at the output of the SMF by

$$U(z,t) = \int_{-\infty}^{\infty} U(0,t')\exp[\,jB(t-t')^2]\mathrm{d}t', \qquad (1)$$

where $B = -1/(2\beta_{2-\mathrm{SMF}}z_{\mathrm{SMF}})$. This FrT can be approximated as a FT under the condition that

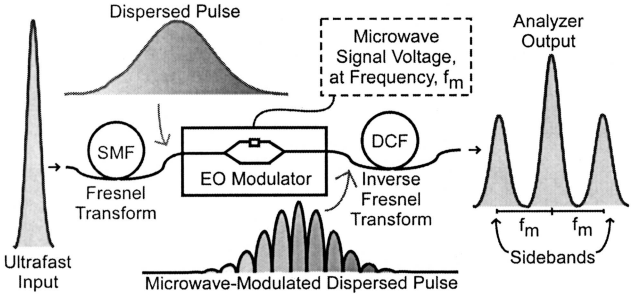


Fig. 1. General microwave analyzer approach to microwave spectrum analysis by use of dispersive fiber for signal processing.

0146-9592/04/050501-03$15.00/0 

$\beta_{2-\mathrm{SMF}} z_{\mathrm{SMF}} \gg \tau^2$, where $\tau$ is the initial, transform-limited pulse width. This requirement is readily satisfied with kilometers of fiber for the few-hundred-femtosecond pulse. Ideal modulation of this dispersion-stretched waveform with a microwave signal, $V(t)$, followed by propagation in DCF to achieve an inverse FrT, leads to a signal:

$$U_c(z,t) = \int_{-\infty}^{\infty} V(t') \int_{-\infty}^{\infty} U(0,t'') \exp[\, jB(t' - t'')^2] \mathrm{d}t'' \times \exp[-jB'(t - t')^2] \mathrm{d}t'. \quad (2)$$

A minimum operable frequency for the microwave signal is set because the period can be no longer than the time window created by the dispersion-broadened optical pulse. To achieve a true inverse FrT with the DCF, $B'$ introduced in Eq. (2) must be equal in magnitude to $B$ used in Eq. (1) for the SMF link. In this analysis we assume that $B' = B = -1/(2\beta_{2-\mathrm{SMF}} z_{\mathrm{SMF}})$; i.e., we ignore the possible mismatch in the dispersion slopes of the fiber. Rearranging terms in Eq. (2) gives

$$U_c(z,t) = \exp(-jBt^2) \int_{-\infty}^{\infty} \times \left\{ \int_{-\infty}^{\infty} \tilde{V}(t') \exp[\, j2B(t - t'')t'] \mathrm{d}t' \right\} U(0,t'') \times \exp(\, jBt''^2) \mathrm{d}t''. \quad (3)$$

Equation (3) contains a FT of the microwave modulating signal in which frequency is mapped to time as $B(t - t'')/\pi$ or $(t - t'')/(2\pi\beta_{2-\mathrm{SMF}} z_{\mathrm{SMF}})$. Completing the first integration, we can rewrite Eq. (3) as

$$U_c(z,t) = \exp(-jBt^2) \int_{-\infty}^{\infty} V[(B/\pi)(t - t'')] \times U(0,t'') \exp(\, jBt''^2) \mathrm{d}t''. \quad (4)$$

The field at the output of the DCF is a convolution of the scaled microwave spectrum with the ultrashort pulse. Note that the second quadratic phase in Eq. (4) can be removed under the approximation that the optical pulse was stretched to and recompressed from the temporal Fraunhofer regime (i.e., $B \ll 1/\tau^2$).

Our experimental setup is an extension of the approach shown in Fig. 1. Ultrafast pulses (150 fs) from a Coherent Mira pumped optical parametric oscillator at 1.56 $\mu$m are dispersed to roughly 1 ns (FWHM) by use of a combination of a grating stretcher and 2.6 km of SMF-28 fiber. The average power launched into the fiber is ~15 mW. The use of the grating stretcher to obtain a small amount of dispersion helps to avoid nonlinearities stemming from the highest peak powers. The modulator, located after the SMF, is a $LiNbO_3$ 10-Gbit/s Mach–Zehnder device with input microwave power levels ranging from 10 to 24 dBm. Following the modulator, system losses require the insertion of an erbium-doped fiber amplifier to boost signal strength. To complete the system, a DCF module offers −44-ps/nm dispersion compensation. The output is viewed by use of an autocorrelator with a scanning delay. Reviewing the scaling of the microwave spectrum in Eq. (3) and inserting $\beta_{2-\mathrm{SMF}} \approx 20$ ps$^2$/km and $z_{\mathrm{SMF}} \approx 2.6$ km into that equation translates time to frequency as 3 GHz/ps in the output trace. A detected plot for a 7-GHz sinusoidal signal is given in Fig. 2(a), where the time axis is converted to frequency by this scaling factor. In the autocorrelation process the dc signal, introduced in practice by the intensity modulator, and the first harmonic contribute to the formation of signal at the second harmonic. Nonlinear modulation enhances the nonlinearity of the system by strengthening the second harmonic and adding higher-order terms. By filtering out the fringe pattern from the interferometric correlation signal in Fig. 2(a) we obtain the intensity correlation shown in Fig. 2(b). Nonlinear modulation is displayed at both 14 and 21 GHz, corresponding to the second and third harmonics, respectively.

To quantify the source of nonlinearity in the system, analysis should include the specifics of the modulation process. The optical field at the output of the DCF is accurately expressed by substitution of $V(t') = \exp(\, j\phi)[1 + \exp(\, j\Gamma)]$ into Eq. (2). Here $\Gamma = b_m + a_m \sin(2\pi f_m t')$ is the voltage applied to the modulator, $b_m$ is the bias voltage, $a_m$ is the amplitude of modulation, and $f_m$ is the frequency of modulation. Rewriting the expression for $V(t')$ with a Fourier series expansion for the last exponential yields

$$V(t') = \exp(-j\phi) \times \left\{ 1 + \sum_{n=-\infty}^{\infty} J_n(a_m) \exp[\, j(b_m + 2\pi n f_m t)] \right\}, \quad (5)$$

where $J_n$ is a Bessel function of the first kind. The modulator is a source of nonlinearity in the system because the device introduces the fundamental microwave frequency $f_m$ in combination with a dc component and higher harmonics. The FT of the microwave signal leads to $\delta$ functions weighted by $J_n(a_m)$ at the dc and all harmonics. Following detection, the output trace will contain a correlation of scaled versions of the ultrafast pulse, $U(0, Bt/\pi)$, when $t = 0$ or when $Bt/\pi = nf_m$.

From inspection of Eq. (5), the factor $J_n(a_m)$ largely controls the linearity of the modulation process. By carefully choosing amplitude $a_m$ of the rf signal in combination with bias voltage $b_m$, one can distribute most

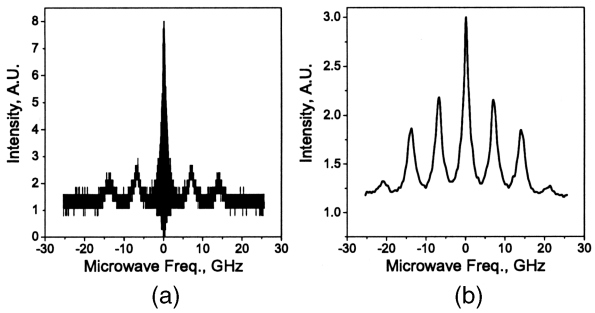


Fig. 2. (a) Interferometric correlation, showing microwave signal at $f_m = 7$ GHz. (b) Intensity correlation reveals the enhancement of second and third harmonics from nonlinear modulation.

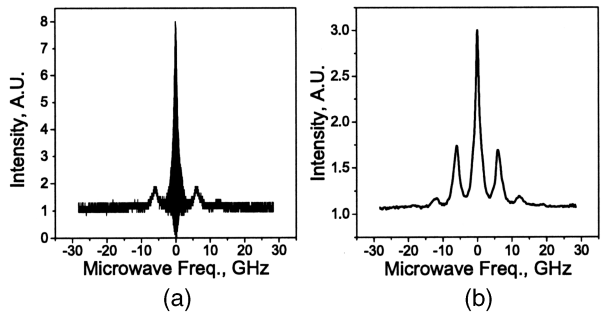


Fig. 3. (a) Interferometric correlation for 6-GHz modulation. (b) Intensity correlation.

of the signal power into the central three pulse locations, i.e., corresponding to the dc and the first harmonic. Shown in Fig. 3(a) is the result of detecting a signal at 6 GHz. Examining the intensity correlation plot [Fig. 3(b)] reveals a very low signal at harmonics above the fundamental modulation frequency.

From the experimental data one can infer that the resolution of the spectrum analyzer is limited by the minimum recompressed pulse width. This temporal width is set by the original launched pulse width and the ability to experimentally match the SMF and the DCF precisely, including dispersion terms higher than second order. In our experiment the launched 150-fs pulse is imaged to an output pulse with an autocorrelation FWHM of 500 fs. Whereas this width sets the resolvable separation between the peaks in the autocorrelation trace, the scaling of time to frequency for the output waveform is governed by the time window created by the broadened pulse between the SMF and the DCF. To elaborate, in our experiment 500 fs corresponds to 1.5 GHz. However, had we stretched the pulse to 100 instead of 1 ns, the same 500 fs would have represented a spectral width of only 15 MHz. A useful figure of merit for spectral analysis techniques is the time–bandwidth product (TBWP) or, alternatively, the number of resolvable spots. In our experimental approach the maximum signal bandwidth and the TBWP are limited by the speed of the EO modulator and the electronic signal generator. Modulator technology has progressed to the point at which modulation in a range of hundreds of gigahertz is possible with polymer-based modulators.[9] Moreover, interactions of optical fields by nonlinear processes may easily extend to modulation in the terahertz range, and our method may help to reveal the nature of these interactions. Fundamentally, the TBWP of our technique is related to the ratio of the duration of the stretched optical pulse, which, as we stated above, defines the period of the lowest microwave frequency, to the recompressed ultrashort pulse width. Using 1 ns as the stretched pulse duration and 500 fs as the recompressed pulse width, we can estimate that the analyzer has of the order of $10^3$ resolvable spots. It can be inferred that adding matched amounts of SMF and DCF to increase dispersive broadening will improve not only the resolution of the spectrum analyzer but also the TBWP. It is evident that the gain in resolution is accompanied by a need for an increased time window of the detector to accommodate the larger temporal shifts.

An important advantage of our technique over conventional electronic methods that rely on high-frequency mixers is the wide instantaneous bandwidth available to the user (i.e., up to terahertz-range bandwidths). Although the scanning delay of the autocorrelation detection technique in our experiment does not take advantage of this wide instantaneous bandwidth, real-time detection is feasible by use of both single-shot detection of ultrafast waveforms and nonlinear time-to-space mapping.[10,11] Such techniques would permit instantaneous access to a multiterahertz signal bandwidth range by exploiting the parallelism of fast spatially arrayed detectors.

In summary, we have introduced and demonstrated experimentally a microwave spectrum analyzer that uses chromatic dispersion in optical fibers as a signal-processing method. Experimental results show good agreement with analytical expectations. Improvement of the system will involve the incorporation of longer segments of matched SMF and DCF to heighten the resolution to the megahertz range. Moreover, our approach can eventually permit switching in longer fiber segments to effectively zoom in on the desired spectral range of a signal. Increasing the number of resolvable spots to the $10^5$ range is predicted.

This research was supported by the Defense Advanced Research Projects Agency, the U.S. Air Force Office of Scientific Research, the National Science Foundation, and Applied Micro Circuits Corporation. D. Panasenko gratefully acknowledges the support of the Fannie and John Hertz Foundation. R. E. Saperstein's e-mail address is res@ece.ucsd.edu.

## References

1. H. Zmuda and E. N. Toughlian, *Photonic Aspects of Modern Radar* (Artech House, Boston, Mass., 1994).
2. B. B. Hu and M. C. Nuss, Opt. Lett. **20,** 1716 (1995).
3. A. J. Seeds, in *International Topical Meeting on Microwave Photonics* (The Institute of Electronics, Information, and Communication Engineers, Tokyo, 2002), pp. 17–20.
4. V. Lavielle, I. Lorgeré, J.-L. Le Gouët, S. Tonda, and D. Dolfi, Opt. Lett. **28,** 384 (2003).
5. J. Chou, Y. Han, and B. Jalali, IEEE Photon. Technol. Lett. **15,** 581 (2003).
6. N. K. Berger, B. Levit, S. Atkins, and B. Fischer, Electron. Lett. **36,** 1644 (2000).
7. B. H. Kolner, IEEE J. Quantum Electron. **30,** 1951 (1994).
8. Y. C. Tong, L. Y. Chan, and H. K. Tsang, Electron. Lett. **33,** 983 (1997).
9. M. Lee, H. E. Katz, C. Erben, D. M. Gill, P. Gopalan, J. D. Heber, and D. J. McGee, Science **298,** 1401 (2002).
10. K. G. Purchase, D. J. Brady, and K. Wagner, Opt. Lett. **18,** 2129 (1993).
11. P. C. Sun, Y. T. Mazurenko, and Y. Fainman, J. Opt. Soc. Am. A **14,** 1159 (1997).